Deactivation of Methylrhenium Trioxide−Peroxide Catalysts by Diverse and Competing Pathways

Mahdi M. Abu-Omar, Peter J. Hansen,† and James H. Espenson*

Contribution from the Ames Laboratory and Department of Chemistry, Iowa State University, Ames, Iowa 50011

Received July 13, 1995. Revised Manuscript Received February 29, 1996[⊗]

Abstract: The peroxides from methylrhenium trioxide (MTO) and hydrogen peroxide, $CH_3ReO_2(\eta^2\text{-}O_2)$, **A**, and $CH_3Re(O)(\eta^2\text{-}O_2)_2(H_2O)$, **B**, have been fully characterized in both organic and aqueous media by spectroscopic means (NMR and UV−vis). In aqueous solution, the equilibrium constants for their formation are $K_1 = 16.1 \pm 0.2$ L mol^{-1} and $K_2 = 132 \pm 2$ L mol^{-1} at pH 0, $\mu = 2.0$ M, and 25 °C. In the presence of hydrogen peroxide the catalyst decomposes to methanol and perrhenate ions with a rate that is dependent on $[H_2O_2]$ and $[H_3O^+]$. The complex peroxide and pH dependences could be explained by one of two possible pathways: attack of either hydroxide on **A** or HO_2^- on MTO. The respective second-order rate constants for these reactions which were deduced from comprehensive kinetic treatments are $k_{\mathbf{A}} = (6.2 \pm 0.3) \times 10^9$ and $k_{\mathrm{MTO}} = (4.1 \pm 0.2) \times 10^8$ L mol^{-1} s^{-1} at $\mu = 0.01$ M and 25 °C. The plot of log k_ψ versus pH for the decomposition reaction is linear with a unit slope in the pH range 1.77−6.50. The diperoxide **B** decomposes much more slowly to yield O_2 and CH_3ReO_3. This is a minor pathway, however, amounting to <1% of the methanol and perrhenate ions produced from the irreversible deactivation at any given pH. Within the limited precision for this rate constant, it appears to vary linearly with $[OH^-]$ with $k = 3 \times 10^{-4}$ s^{-1} at pH 3.21, $\mu = 0.10$ M, and 25 °C. Without peroxide, CH_3ReO_3 is stable below pH 7, but decomposes in alkaline aqueous solution to yield CH_4 and ReO_4^-. As a consequence, the decomposition rate rises sharply with $[H_2O_2]$, peaking at the concentration at which [**A**] is a maximum, and then falling to a much smaller value. Variable-temperature ^{1}H NMR experiments revealed the presence of a labile coordinated water in **B**, but supported the anhydride form for **A**.

Introduction

Methylrhenium trioxide (CH_3ReO_3, MTO) catalyzes a broad spectrum of oxygen atom transfer reactions. It commonly assists in the transfer of an O atom from hydrogen peroxide to a suitable substrate, **S**, as represented by the following generalized chemical equation:

$$\mathbf{S} + H_2O_2 \xrightarrow{\text{cat. MTO}} SO + H_2O \qquad (1)$$

A wide range of substrates can participate in this reaction: alkenes,[1,2] phosphines,[3] sulfides,[4] metal thiolate complexes,[5] bromide ions,[6] amines,[7] and so on. We and others are studying how MTO functions as a catalyst. We must also define any limitations to its use. Two catalytically-active peroxorhenium complexes, with 1:1 and 2:1 peroxide:rhenium ratios, are involved. They are $CH_3Re(O)_2(\eta^2\text{-}O_2)$ (**A**) and $CH_3Re(O)(\eta^2\text{-}O_2)_2(H_2O)$ (**B**). We address here not the catalytic reactions per se, but solvolytic and other reactions that the peroxorhenium complexes undergo on their own, which lead to deactivation of MTO.

Alone in water and in mixed aqueous−organic solvents, dilute solutions of CH_3ReO_3 persist for days with minimal (<5%) decomposition. When CH_3ReO_3 and H_2O_2 are present together, however, decomposition ensues, usually over the course of a few hours, depending on the peroxide concentration and the pH. Generally speaking, the system is more stable against decomposition at high $[H_3O^+]$. In organic solvents, however, **B** is stable at ambient temperature provided hydrogen peroxide is in excess. We thus undertook a study of how this catalytic system decomposes in an aqueous medium. Over time, both methanol and oxygen can be detected, and both methylrhenium trioxide and hydrogen peroxide decrease in concentration. Others have claimed[8] that the products form together, and have described the major decomposition pathway by the following equation:

$$CH_3Re(O)(\eta^2\text{-}O_2)_2(H_2O) \xrightarrow{?} CH_3OH + H[ReO_4] + {}^1/_2O_2 \qquad (2)$$

We shall see, however, that eq 2 is not a correct representation of the deactivation processes; oxygen is a minor byproduct compared to methanol and perrhenate ions.

In the early stages of this investigation it became evident that an array of methods would be needed to characterize the chemical events taking place. We have employed several experimental techniques: ^{1}H NMR, stopped-flow, oxygen-sensing electrodes, UV−vis spectroscopy, kinetics, and gas chromatography.

As it turns out, the decomposition reactions in the MTO−H_2O_2 system are of interest in their own right, independent of their implications for catalyst stability. These reactions speak to the different modes by which peroxo−metal complexes can react, a subject that has commanded considerable independent interest.[9,10]

† On leave from Northwestern College, Orange City, IA.

[⊗] Abstract published in *Advance ACS Abstracts,* May 1, 1996.

(1) Herrmann, W. A.; Fischer, R. W.; Marz, D. W. *Angew. Chem., Int. Ed. Engl.* **1991**, *30*, 1638.
(2) Al-Ajlouni, A.; Espenson, J. H. *J. Am. Chem. Soc.* **1995**, *117*, 9243.
(3) Abu-Omar, M. M.; Espenson, J. H. *J. Am. Chem. Soc.* **1995**, *117*, 272.
(4) Vassell, K. A.; Espenson, J. H. *Inorg. Chem.* **1994**, *33*, 5491.
(5) Huston, P.; Espenson, J. H.; Bakac, A. *Inorg. Chem.* **1993**, *32*, 4517.
(6) Espenson, J. H.; Pestovsky, O.; Huston, P.; Staudt, S. *J. Am. Chem. Soc.* **1994**, *116*, 2869.
(7) Zhu, Z.; Espenson, J. H. *J. Org. Chem.* **1995**, *60*, 1326.
(8) Herrmann, W. A.; Fischer, R. W.; Rauch, M. U.; Scherer, W. *J. Mol. Catal.* **1994**, *86*, 243.
(9) Ledon, H.; Bonnet, M.; Lallemand, J.-Y. *J. Chem. Soc., Chem. Commun.* **1979**, 702.

S0002-7863(95)02305-5 CCC: $12.00

In addition, **A** was further characterized spectroscopically. We sought to resolve the issue of whether **A**, like **B**, has a water molecule coordinated to rhenium. Also, the equilibrium constants for peroxide binding and the spectrum of **A** were determined more precisely.

Experimental Section

Materials. HPLC grade tetrahydrofuran (Fisher) was used, and high-purity water was obtained by passing laboratory-distilled water through a Millipore-Q water purification system. Hydrogen peroxide solutions, prepared by diluting 30% H_2O_2 (Fisher), were standardized by iodometric titration. The purity of starting reagents was checked by ^{1}H NMR.

Methylrhenium trioxide was prepared by a literature method[11] or purchased from Aldrich. Stock solutions of CH_3ReO_3 were prepared in water, protected from light, and stored at −5 °C. The solutions were used within 3 days. Their concentrations were determined spectrophotometrically prior to each use.[12] Labeled hydrogen peroxide-^{18}O was purchased from ICON Services, Inc., as a 1.4% solution in $H_2{}^{16}O$, and 94% $H_2{}^{18}O$ from ISOTEC, Inc.

Instrumentation. ^{1}H NMR spectra were obtained with either a Nicolet 300 MHz or a Varian VXR-300 spectrometer. NMR spectra recorded in THF-d_8 were referenced to Me_4Si. *tert*-Butyl alcohol (δ 1.27) was used as an internal reference for spectra obtained in D_2O.[13] For spectrophotometric measurements, conventional (Shimadzu UV-2101PC and UV-3101PC) and stopped-flow (Sequential DX-17MV, Applied Photophysics Ltd.) instruments were used with quartz cells (1 or 2 cm optical path length). The pH was measured using a Corning pH meter, model 320. Molecular oxygen production was measured using a YSI Model 5300 biological oxygen monitor with a Model 5331 oxygen probe. All measurements were made at 25.0 ± 0.2 °C, and the instrument was calibrated using air-saturated water assuming $[O_2] = 0.27$ mM.[14] Methane production was measured with an HP 5790A Series gas chromatograph using an Alltech VZ-10 packed column and an HP 3390A integrator. Electrospray mass spectra of perrhenate were obtained using a Finnigan TSQ 700 operated in the single quad mode for negative ions.

Results

Identification of A by NMR. The chemical shift of **A** in THF-d_8 was recently reported to be 3.2 ppm.[15] When we mixed equimolar amounts of MTO and H_2O_2 (50 mM each) in THF-d_8 and recorded the ^{1}H NMR spectrum, three CH_3 signals were apparent: $\delta(CH_3) = 2.1$ (MTO), 2.4 (**A**), and 3.3 (CH_3OH, from partial decomposition) ppm. The peak of **A** at 2.4 ppm increased with time, as did the methanol signal at 3.3 ppm, although at different rates. When more hydrogen peroxide was added to this solution (10× the initial MTO concentration), the peaks of MTO and **A** diminished and a new peak emerged at 2.7 ppm, corresponding to the di(η^2-peroxo) complex **B**. The signal for methanol did not continue to increase once **A** and MTO were converted to **B** by the addition of a sufficiently high concentration of hydrogen peroxide. We infer that the first-reported[15] chemical shift of **A** was in fact that of the methanol formed by partial decomposition.

The rates of formation of **A** and **B** in THF depend on the water concentration; the source of water in this experiment was the 30% H_2O_2. Drying H_2O_2 solutions in THF proved difficult, since the formation of **A** and **B** yields water, free or coordinated. Hence, complete exclusion of water was not attempted; the amount of water present, however, was limited to that introduced by the 30% H_2O_2. Figure 1 shows the time profile for the formation of **A** (2.4 ppm) from MTO (2.1 ppm) in THF-d_8 from an equimolar mixture of MTO and H_2O_2 (50 mM). The curve for **A** constitutes a rise-and-fall pattern according to which **A** first forms from MTO and H_2O_2, and then the [**A**] drops as MeOH (3.3 ppm) is produced from catalyst degradation. In THF, the pseudo-first-order rate constant for the formation of **A** is $(3.7 \pm 0.2) \times 10^{-3}$ s^{-1}, and that for its decomposition is $(3.1 \pm 0.3) \times 10^{-4}$ s^{-1}.

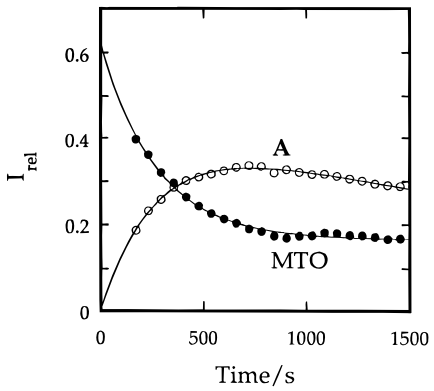

Figure 1. Kinetic traces obtained by NMR spectroscopy for the formation of **A** in THF-d_8. Conditions: $[MTO] = [H_2O_2] = 50$ mM at 25.0 °C. The fit for **A** is based on the model MTO + $H_2O_2 \rightarrow$ **A** $\rightarrow$ MeOH + H^+ + ReO_4^-.

At high $[H_2O_2]$, where **A** forms very rapidly, the reaction of **A** with one additional mole of peroxide to form **B** could also be followed by ^{1}H NMR. The first-order rate constant for the formation of **B** from **A** in THF-d_8 with 40 mM MTO and 0.30 M H_2O_2 is $(2.05 \pm 0.04) \times 10^{-3}$ s^{-1}.

Is Water Coordinated to A and B? This issue was examined by variable-temperature ^{1}H NMR. Solutions of H_2O_2 in THF-d_8 were dried over $MgSO_4$. Although fully-dried peroxide was not obtained, the water concentration was quite significantly reduced. In one set of conditions, high $[H_2O_2] =$ 1.0 M and $[MTO] = 0.08$ M were used, so that only **B** would be present. The temperature was varied from +20 °C to −55 °C. At −40 °C two water peaks were evident, one for free water at 5.3 ppm and the other at 6.2 ppm for coordinated water. As shown in Figure 2, the two are well separated. The low temperature was needed to separate the coordinated water peak from that of free water, since this water is reasonably labile. This finding contradicts another report,[15] wherein water is said to be tightly bound to **B** and not exchanging, with a chemical shift of 9.4 ppm. We found no chemical shift that high in the variable-temperature NMR experiments. In general, we find that the peaks broadened and coalesced as the temperature was raised. The rate of water exchange proved to be dependent on the concentration of water, consistent with the following exchange process:

$$CH_3Re(O)(\eta^2\text{-}O_2)_2(H_2O) + H_2O^* \rightleftarrows CH_3Re(O)(\eta^2\text{-}O_2)_2(H_2O^*) + H_2O \quad (3)$$

A second set of experiments employed a low $[H_2O_2] = 80$ mM and $[MTO] = 80$ mM to give a solution containing predominantly **A** and MTO and little **B**. The temperature was again varied from +20 °C to −55 °C. The separation of a coordinated water peak for **A** was not observed. We conclude, therefore, either that **A** lacks a coordinated water or that its

(10) Brown, S. N.; Mayer, J. M. *Inorg. Chem.* **1992**, *31*, 4091.
(11) Herrmann, W. A.; Kühn, F. E.; Fischer, R. W.; Thiel, W. R.; Ramao, C. C. *Inorg. Chem.* **1992**, *31*, 4431.
(12) Kunkely, H.; Turk, T.; Teixeira, C.; Bellefon, C. d. M. d.; Herrmann, W. A.; Volger., A. *Organometallics* **1991**, *10*, 2090.
(13) Gordon, A. J.; Ford, R. A. *The Chemist's Companion*; Wiley: New York, 1972.
(14) Fogg, P. C. T.; Gerrard, W. *Solubility of Gases in Liquids*; Wiley: New York, 1991; p 293.
(15) Herrmann, W. A.; Fischer, R. W.; Scherer, W.; Rauch, M. H. *Angew. Chem., Int. Ed. Engl.* **1993**, *32*, 1157.

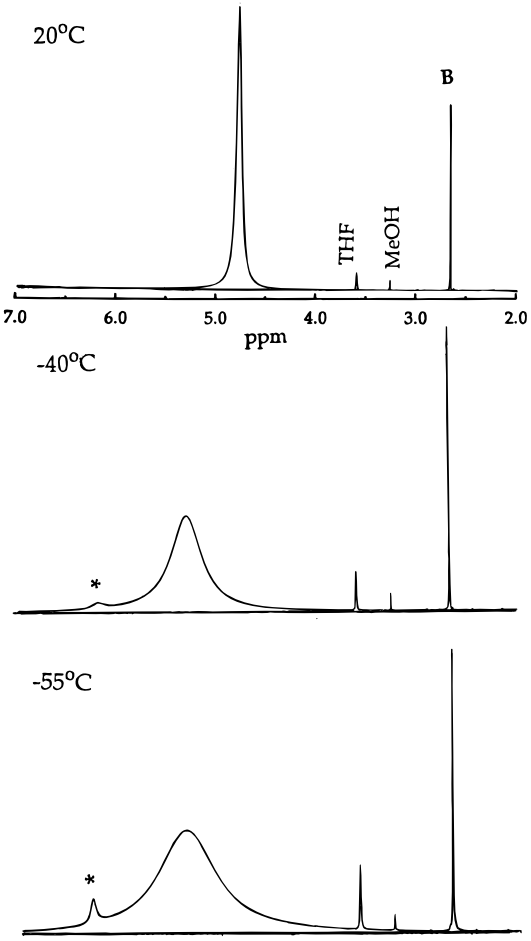

Figure 2. Variable-temperature ^{1}H NMR spectra of **B** (generated in situ) in THF-d^8. Conditions: 80 mM MTO and 1.0 M H_2O_2. The asterisk indicates coordinated H_2O.

coordinated water is much more labile than that of **B**. Because of other results from the pH-dependent kinetics, as presented in a later section, we are inclined to the first interpretation.

Catalyst Deactivation. General Observations. Compound **B** is stable in organic solvents including tetrahydrofuran, acetonitrile, and acetone, especially with excess peroxide. In aqueous solutions, however, the peroxides are prone to decompose, although the addition of acid greatly improves their stability. NMR experiments in THF-d_8, similar to the ones described previously, revealed that, at low peroxide (generally $\leq$[Re_{tot}], such that [**A**] $\gg$ [**B**]), methanol is the decomposition product. Perrhenate ions were detected from the distinctive UV band at 225 nm after decomposing the interfering hydrogen peroxide by adding NaOH and heating to 100 °C or by adding MnO_2. Perrhenate ions were also detected by their distinctive UV absorption without the need to decompose hydrogen peroxide when [H_2O_2] was low enough, that is $\leq$5 mM. Hence, methanol and perrhenate ions are formed concurrently by either one of the following net reactions:

$$CH_3Re(O)_2(\eta^2\text{-}O_2) + H_2O \rightarrow CH_3OH + H^+ + ReO_4^- \quad (4)$$

$$CH_3ReO_3 + HO_2^- \rightarrow CH_3OH + ReO_4^- \quad (5)$$

Even under acidic aqueous conditions the same reaction occurred, albeit more slowly. On the basis of the equilibrium constants for peroxide binding (K_1 and K_2 were determined here as subsequently described), we settled on conditions where there

Scheme 1

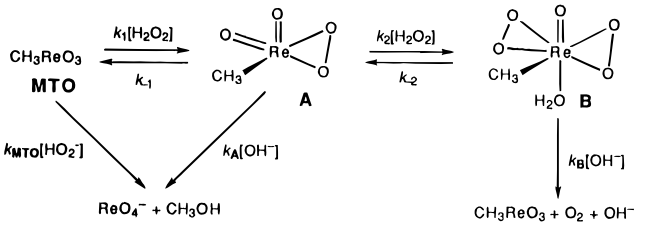

are comparable concentrations of all three rhenium species, for example, 60 mM MTO, 70 mM H_2O_2, and 1.0 M $DClO_4$ in D_2O. The ^{1}H NMR spectrum was run as soon as practicable (ca. 4 min after mixing). Along with a substantial amount of CH_3OD (δ 3.4 ppm), the spectrum showed MTO (δ 2.5), **A** (δ 2.6), and **B** (δ 3.0) in ratios that agree with those predicted from the equilibrium constants.

When this experiment was repeated with a large excess of H_2O_2, **B** was the only methylrhenium compound detected, and little methanol was seen.

Catalyst Decomposition. Kinetics. This system is sufficiently intricate in its pattern of kinetic behavior that it seems worthwhile to display all the plausible reactions before presenting the data from which they were constructed. The reactions are given in Scheme 1.

The two reactions in Scheme 1 that account for the production of methanol and perrhenate ions are kinetically indistinguishable, since they both give rise to an identical transition state, namely, $[CH_3ReO_5H^-]^{\ddagger}$. The rate equations for this scheme will be written so as to presume the two peroxide binding steps are sufficiently rapid that they can be treated as prior equilibria, a point that we verified independently. It should be noted from this scheme that the irreversible decomposition of the catalyst proceeds via the reaction of either **A** with hydroxide or MTO with HO_2^-, whereas **B** regenerates MTO upon expulsion of dioxygen. The kinetic equations for Scheme 1 will be derived here, since we are not aware of a prior derivation. Let C_t represent at any time t the concentration of all the forms of rhenium other than perrhenate ions:

$$[Re]_T = C_t + [ReO_4^-]_t \quad (6)$$

By differentiating this equation, and assuming perrhenate ions originate from **A** only, we have

$$\frac{d[ReO_4^-]}{dt} = -\frac{dC}{dt} = k_{\mathbf{A}}[\mathbf{A}][OH^-] = k_{\mathbf{A}}f_{\mathbf{A}}[OH^-]C_t \quad (7)$$

where $f_{\mathbf{A}} = [\mathbf{A}]_t/C_t$ is given by

$$f_{\mathbf{A}} = \frac{K_1[H_2O_2]}{1 + K_1[H_2O_2] + K_1K_2[H_2O_2]^2} \quad (8)$$

Integration of this equation, noting that $C_0 = [Re]_T$, affords

$$C_t = [Re]_T \exp(-k_{\mathbf{A}}f_{\mathbf{A}}[OH^-]t) \quad (9)$$

On the other hand, assuming perrhenate ions instead originate from the reaction of MTO and HO_2^-, we obtain

$$\frac{d[ReO_4^-]}{dt} = -\frac{dC}{dt} = k_{MTO}[MTO][HO_2^-] = k_{MTO}f_{MTO}[HO_2^-]C_t \quad (10)$$

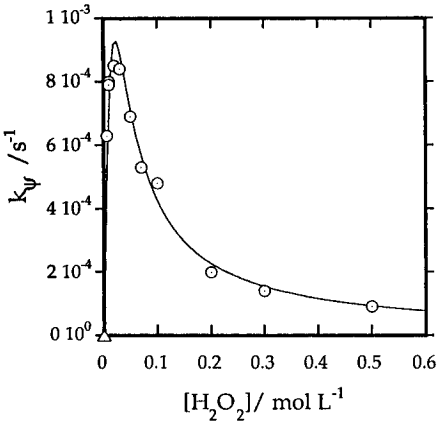

Figure 3. Pseudo-first-order rate constant for the decomposition of the catalyst as a function of $[H_2O_2]$. The fit to eq 9 (or to the integral of eq 10) yields $k_A[OH^-]$ (or $(k_{MTO}K_a^{H_2O_2}/K_1K_w)[OH^-]$) = 0.0062 ± 0.0003 s^{-1}. Conditions: 1.0 mM MTO, 0.010−0.50 M H_2O_2, and μ = $[HClO_4]$ = 0.010 M at 25.0 °C.

where $f_{MTO} = [MTO]_t/C_t$ is given by

$$f_{MTO} = \frac{1}{1 + K_1[H_2O_2] + K_1K_2[H_2O_2]^2} \tag{11}$$

and $[HO_2^-]$ expressed relative to $[H_2O_2]$ is

$$[HO_2^-] = \frac{K_a^{H_2O_2}[OH^-][H_2O_2]}{K_w} \tag{12}$$

Therefore, eqs 7 and 10 differ only in the identities of the equilibrium and rate constants while maintaining the same dependences on hydrogen peroxide, hydroxide, and rhenium concentrations. In summary, both methanol-producing reactions in Scheme 1 give rise to indistinguishable rate laws as shown by eqs 7 and 10. This treatment accounts for the main pathway following first-order kinetics at constant pH and at constant f_A or f_{MTO}, which also implies at constant $[H_2O_2]$, by virtue of it being taken in excess.

The quantitative kinetic study of the decomposition pathways was carried out spectrophotometrically by monitoring the absorbance at 360 nm, where **A** and especially **B** (ϵ_{max} = 1.1 × 10^3 L mol^{-1} cm^{-1}) absorb. In an extensive series of experiments $[Re]_T$ was maintained at 1.00 mM and the pH at 2.0 with perchloric acid. The concentration of hydrogen peroxide was varied in the range 0.007−0.50 M. The data from each experiment followed first-order kinetics, and the value of k_ψ was evaluated from nonlinear least-squares fitting of the absorbance−time curves to a single exponential function.

A plot of k_ψ versus $[H_2O_2]$ was made, as shown in Figure 3. The rate constant rises from very near zero without peroxide, and after peaking it falls, following the proportion of **A**. According to eqs 7, 8, and 10−12. The fit to eq 9 yielded $k_A[OH^-]$ = (6.2 ± 0.3) × 10^{-3} s^{-1} or $k_{MTO}[OH^-]$ = (4.1 ± 0.2) × 10^{-4} s^{-1} at pH 2.00 and μ = 0.01 M.

As shown in Scheme 1, **B** decomposes to yield O_2. Again from this scheme the rate of buildup of oxygen, for the moment using k'_B to symbolize the rate constant at a particular pH, is given by

$$d[O_2]/dt = k'_B[B] = f_B k'_B C_t = f_B k'_B [Re]_T e^{-f_A k_A [OH^-] t} \tag{13}$$

where

$$f_B = \frac{K_1K_2[H_2O_2]^2}{1 + K_1[H_2O_2] + K_1K_2[H_2O_2]^2} \tag{14}$$

Since $k_A[OH^-] = k_\psi/f_A$, regardless of whether k_ψ is measured spectrophotometrically or from O_2 buildup, the value of k_B' can be obtained from the yield of oxygen at the end of the reaction. Integration of eq 13 and rearrangement afford the expression

$$k_B' = \frac{f_A k_A [OH^-]}{f_B} \frac{[O_2]_\infty}{[Re]_T} \tag{15}$$

Similar expressions, of course, could be written using the MTO and HO_2^- reaction as the decomposition pathway by relating k_A to k_{MTO} as shown in the following relation:

$$k_A = \frac{k_{MTO}K_a^{H_2O_2}}{K_1K_w} \tag{16}$$

The overall relationship between k'_B and $[O_2]$ remains unchanged. The only difference lies in expressions of rate and equilibrium constants for the formation of methanol and perrhenate.

Oxygen buildup, detected with an oxygen electrode, was used to monitor the decomposition processes at high $[H_2O_2]$, 0.2−0.8 M. These experiments had $[Re]_T$ = 1.00 mM at pH 3.21 (H_3PO_4/KH_2PO_4 buffer) and 25 °C. The final O_2 concentration varied linearly with $[H_2O_2]$, and the plot of k_ψ shows a hyperbolic dependence on $[H_2O_2]$. These relationships are depicted in Figure 4. Since the expression for f_A at high $[H_2O_2]$ reduces to $f_A = f_A/f_B = 1/K_2[H_2O_2]$, these forms are expected from, and are consistent with, Scheme 1. The average value of k_B at pH 3.21 and μ = 0.10 M is (2.9 ± 0.6) × 10^{-4} s^{-1}. Increasing $[H_2O_2]$ results in an increased ratio of **B** to **A** and MTO, thus enhancing the relative importance of the O_2-producing reaction of **B**. At the same time, however, the destruction of the catalyst is slowed since **A** decomposes irreversibly. Nonetheless, decomposition of **B** is minor (<1%) compared to the irreversible decomposition leading to methanol and perrhenate ions. This means that the kinetic data for this very minor pathway are of considerably lower quality; this point must be kept in mind in considering the data obtained.

The results of these experiments are given in Table 1, which includes values of the rate constants that were calculated from values of K_1 and K_2 determined at pH 0 (see later). The peroxide-binding equilibria are not noticeably pH-dependent, and this treatment should be fully reliable.

The possibility was considered that methane formation might accompany the decomposition of **B**:

$$CH_3Re(O)(\eta^2\text{-}O_2)_2(H_2O) \rightarrow CH_4 + H^+ + ReO_4^- + O_2\ (?) \tag{17}$$

Although this would yield stable products, we reject this alternative on the basis of the results of GC analyses for methane. Only a trace of CH_4 could be detected from a reaction between MTO (1.0 mM) and H_2O_2 (0.8 M) at pH 3.21. It amounted to only 2.2(±0.3)% of the amount of O_2 formed under these conditions, after calibration of the GC with pure methane from the decomposition of MTO in NaOH solutions (see later).

Catalyst Decomposition. pH Profile. The kinetic dependence of the rate of decomposition on $[H_3O^+]$ was investigated with $[Re]_T$ = 0.10 mM and at $[H_2O_2]$ = 2.00 mM to maximize the accuracy. At this concentration f_A reduces to $f_A = K_1[H_2O_2]$, and k_ψ to $k_A[OH^-]K_1[H_2O_2]$ or to $(k_{MTO}K_a^{H_2O_2}/K_w)[OH^-]$-

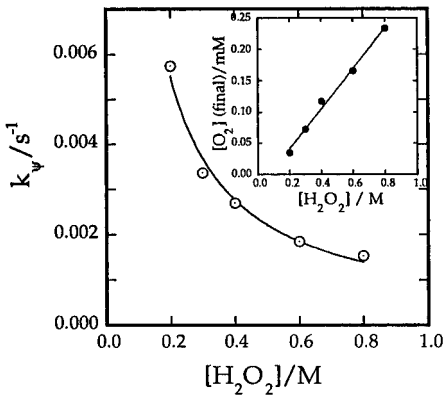

Figure 4. Pseudo-first-order rate constant from O_2 measurements as a function of [H_2O_2]. Conditions: 1.0 mM MTO, 0.2−0.8 M H_2O_2, pH 3.21, μ = 0.10 M at 25.0 °C. Inset: Linear relationship between the amount of O_2 produced and the [H_2O_2] as required by eq 18.

Table 1. Kinetic Results and Yields from the Measurement of O_2 Production[a]

[H_2O_2]/ M	k_ψ/ (10^{-3} s^{-1})	[O_2]$_\infty$/ mM	k'_A/s^{-1}	k'_B/ (10^{-4} s^{-1})	f_A	f_B
0.20	5.7	0.035	0.16	2.1	0.036	0.95
0.30	3.4	0.073	0.14	2.5	0.025	0.97
0.40	2.7	0.12	0.14	3.2	0.019	0.98
0.60	1.8	0.17	0.15	3.1	0.013	0.99
0.80	1.5	0.23	0.16	3.6	0.0094	0.99
			av: 0.15	2.9×10^{-4}		

[a] Experimental conditions: 1.0 mM MTO, pH 3.21 (H_3PO_4/KH_2PO_4 buffer), and μ = 0.10 M at 25 °C. The f_A and f_B values were calculated with K_1 = 16.1 L mol^{-1} and K_2 = 132 L mol^{-1}.

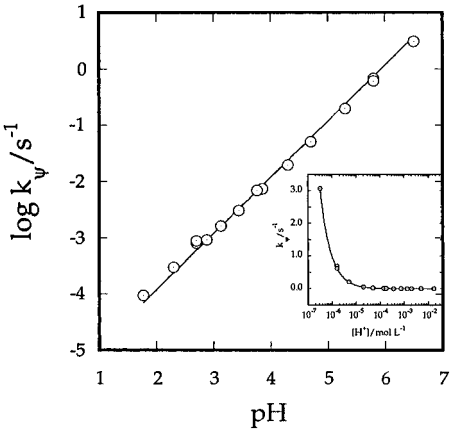

Figure 5. k_ψ for the irreversible decomposition reaction as a function of pH. Conditions: 0.10 mM MTO, 2.0 mM H_2O_2, and μ = 0.05 M at 25.0 °C. Inset: k_ψ versus [H^+] (log scale). The fit shown is that to $k_\psi = k'/[H^+]$.

[H_2O_2] (refer to eqs 7, 8, and 16). For each of 15 experiments a constant pH was maintained using $HClO_4$ (pH < 3), or one of a series of buffers, H_3PO_4/KH_2PO_4 (pH 2.9−3.8), HOAc/NaOAc (pH 3.8−5.8), or KH_2PO_4/K_2HPO_4 (pH 5.8−6.8). A constant ionic strength of 0.050 M was maintained with lithium perchlorate.

The pH profile (log k_ψ versus pH), shown in Figure 5, is linear with a slope of 0.95 ± 0.01. The inset shows the fitting of k_ψ directly to the expression $k_\psi = k'/[H_3O^+]$. The value of k' is (9.76 ± 0.06) × 10^{-7} mol L^{-1} s^{-1}, and therefore k_A = 3.05 × 10^9 L mol^{-1} s^{-1} and k_{MTO} = 2.03 × 10^8 L mol^{-1} s^{-1} at μ = 0.050 M. For now, we simply take this to be the basis on which the decomposition of the catalyst in Scheme 1 is written with a direct dependence upon [OH^-]. The molecular basis for this chemistry will be presented in the Discussion.

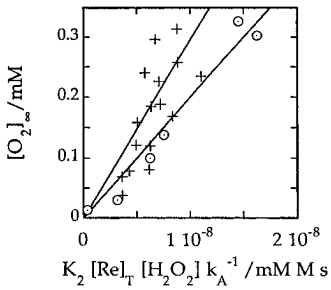

Figure 6. [O_2]$_\infty$ as a function of (K_2[Re]$_T$[H_2O_2])/k_A (see eq 18). Conditions: 1.0 mM MTO, 0.15−1.00 M H_2O_2, pH 2.6−3.5 (H_3PO_4/KH_2PO_4 buffer), 25.0 ± 0.2 °C, μ = 0.10 M (+), 0.20 M (○).

The pH profile for decomposition of **B** is harder to define with certainty, since so little decomposition leads to oxygen. The conclusion we have reached is that **B** probably reacts with a first-order dependence on [OH^-], just like **A** and MTO do. Rearrangement of eq 15, after substitution of the expressions for f_A and f_B, affords the following relation between [O_2]$_\infty$ and [H_2O_2]:

$$[O_2]_\infty = \frac{k'_B}{[OH^-]} \frac{K_2[Re]_T[H_2O_2]}{k_A} \quad (18)$$

The plot suggested by this equation, [O_2]$_\infty$ versus K_2[Re]$_T$-[H_2O_2]/k_A, where each individual k_A value and not the average was taken, is shown in Figure 6 for data taken at two ionic strengths, 0.1 and 0.2 M. Each of the plots approximates a straight line, but the precision is evidently fairly low. Again, this reflects the fact that oxygen evolution is a quite minor pathway. At any rate, within the precision of the data, the values determined over the accessible pH interval (2.6−3.5) fall on a straight line, indicating that the slope is roughly pH-independent. For that to be the case, the denominator term in [OH^-] must be canceled by a corresponding term in the numerator, or $k'_B = k_B[OH^-]$. The values of k_B are (3.0 ± 0.2) × 10^7 and (2.0 ± 0.1) × 10^7 L mol^{-1} s^{-1}, at μ = 0.10 and 0.20 M, respectively.

Labeling Studies. Since all the kinetic data presented thus far for the irreversible decomposition reaction could be rationalized by either the reaction of HO_2^- upon MTO or that of hydroxide upon **A**, we carried out labeling experiments utilizing ^{18}O enriched hydrogen peroxide and water in an effort to distinguish between the two pathways. The reaction of **A** with hydroxide ions would result in the incorporation of two peroxide oxygens into the final perrhenate ions (eq 20); on the other hand, if MTO reacts with HO_2^- and a peroxide oxygen is used to form MeOH, then only one peroxide oxygen would remain on the final perrhenate (eq 19). It is worth noting here that the peroxide oxygens of **A** and **B** in this catalytic system exchange with neither the oxo ligands on the rhenium nor with water molecules.

$$CH_3ReO_3 + H^{18}O^{18}O^- \xrightarrow{?} ReO_3{}^{18}O^- + CH_3{}^{18}OH \quad (19)$$

$$CH_3ReO_2(\eta^2\text{-}{}^{18}O_2) + HO^- \xrightarrow{?} ReO_2{}^{18}O_2{}^- + CH_3OH \quad (20)$$

The perrhenate ions from catalyst decomposition were isolated as the potassium salt. A 15 mg (60 μmol) sample of MTO was dissolved in 0.60 mL of H_2O^{16} containing 6 mg (60 μmol) of $KHCO_3$. A 120 μL sample of 1.5% $H_2{}^{18}O_2$ (90% ^{18}O enrichment) was added and the mixture allowed to stir for a few minutes to ensure complete decomposition. The presence of bicarbonate is necessary to neutralize the produced perrhenic

(16) Murmann, R. K. *J. Phys. Chem.* **1967**, *71*, 974.

Scheme 2

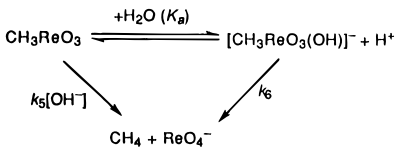

acid, since the perrhenate oxygen exchange reaction is very rapid at acidic pHs.[16]

The solvent was removed under vacuum and the resulting $KReO_4$ collected. The $KReO_4$ was dissolved in methanol and the mass of the anion determined. A similar experiment was performed by labeling the MTO oxygens with $H_2{}^{18}O$ and using unlabeled $H_2{}^{16}O_2$.

The major perrhenate species detected by electrospray mass spectrometry corresponded to the fully exchanged anion, that is, $Re^{18}O_4^-$ in the case of using $H_2{}^{18}O/H_2{}^{16}O_2$ and $Re^{16}O_4^-$ when $H_2{}^{16}O/H_2{}^{18}O_2$ are used. Evidently, the oxygen exchange between the produced ReO_4^- and water[16] made these labeling experiments inconclusive with regards to resolving the true pathway of decomposition.

Decomposition of MTO Itself. MTO is known to decompose to CH_4 and ReO_4^- in alkaline solutions, and was assumed to proceed via a hydroxide ion adduct.[17,18] We monitored the rate of eq 21 by both ^1H NMR and UV−vis methods.

$$CH_3ReO_3 + OH^- \rightarrow CH_4 + ReO_4^- \qquad (21)$$

Addition of NaOH to 50 mM MTO in D_2O resulted in an immediate color change from clear to yellow, followed by gas evolution over a period of time. The NMR peak of MTO (δ 2.5 ppm) shifted to 1.9 ppm, and then disappeared after several hours. The UV−vis spectrum of 0.1 mM MTO changed immediately with 30 mM NaOH. The new yellow compound displays an absorption maximum at 340 nm ($\epsilon = 1500$ L mol^{-1} cm^{-1}). This lends support to the existence of an intermediate, as presented in Scheme 2.

The dependence of the experimental reaction rate upon [OH^-] is shown in Figure 7. The experimental conditions were as follows: 0.20 mM MTO, 0.0050−0.70 M NaOH, and $\mu = 1.0$ M ($LiClO_4$) at 25.0 °C. The kinetic scheme gives the rate law

$$v = \frac{(k_5K_w + k_6K_a)[OH^-]}{K_w + K_a[OH^-]}[Re]_T \qquad (22)$$

A nonlinear least squares fit gives $K_a = (1.2 \pm 0.2) \times 10^{-12}$ mol L^{-1} and $(k_5K_w + k_6K_a) = 2.7 \times 10^{-16}$ mol L^{-1} s^{-1}. The matter cannot be resolved further on the basis of kinetic data unless one assumes that only the k_5 path is important (giving $k_5 = (2.7 \pm 0.3) \times 10^{-2}$ L mol^{-1} s^{-1}), or the obverse, in which case $k_6 = (2.23 \pm 0.06) \times 10^{-4}$ s^{-1}. The value of K_a for MTO at 25 °C and $\mu = 1.0$ M was confirmed by a spectrophotometric titration of MTO and NaOH; measured absorbances at 360 and 390 nm yield an average K_a of 2.2×10^{-12} mol L^{-1}.

Equilibrium Constants for Peroxide Coordination. The equilibrium constants for the formation of **A** and **B** in aqueous solution were determined at 25.0 °C. These are the values of K_1 and K_2 from Scheme 1. The solutions contained 1.0 M $HClO_4$, 1.0 M $LiClO_4$, 0.74 mM MTO, and variable [H_2O_2], 0.0071−0.22 M. The spectra of 15 such solutions were recorded in the range 280−420 nm at intervals of 0.2 nm. The absorbance readings were fit globally using the program SPECFIT.[19] The known spectra of MTO and H_2O_2 were entered and held constant. This fitting gives $K_1 = 16.1 \pm 0.2$ L mol^{-1} and $K_2 = 132 \pm 2$ L mol^{-1}. The calculated spectra of **A** and **B** are shown in Figure 8.

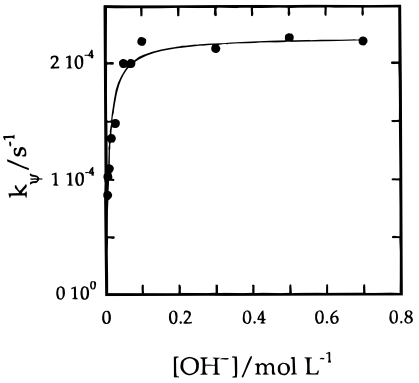

Figure 7. Pseudo-first-order rate constants in alkaline solution for the decomposition of MTO to CH_4 and ReO_4^-. Conditions: 0.20 mM MTO, 0.0050−0.70 M OH^-, and $\mu = 1.0$ M ($LiClO_4$) at 25.0 °C.

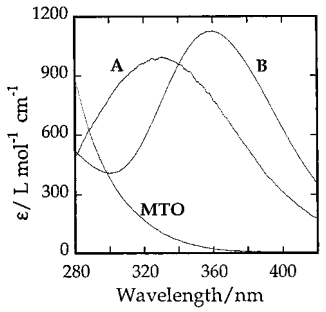

Figure 8. Spectra of **A** and **B** obtained from SPECFIT fitting shown alongside that of MTO in the range 280−420 nm.

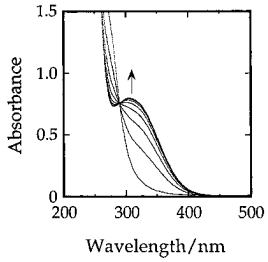

Figure 9. Repetitive spectral changes at 60 min intervals for the formation of **A** from 1.0 mM MTO and 0.010 M H_2O_2 in THF at 25.0 ± 0.2 °C.

Timed repetitive scan spectra were also taken at a fixed [H_2O_2] = 10 mM and [MTO] = 1.0 mM in THF. The overlaid spectra, Figure 9, feature an isosbestic point at 290 nm, indicating that no intermediates attain an appreciable concentration. In THF, **A** has a maximum at 305 nm ($\epsilon = 730$ L mol^{-1} cm^{-1} compared to a literature value[15] of $\epsilon = 600$ L mol^{-1} cm^{-1}). Addition of 0.47 M H_2O increased the rate at which **A** formed. The decomposition of the catalyst is also accelerated by water.

Repetitive scan spectra for the formation of **B** from MTO via **A** show the expected two stages, Figure 10. The concentrations were [MTO] = 1.0 mM and [H_2O_2] = 0.20 M. Following formation of **A**, the repetitive spectra show an isosbestic point for **A** and **B** at 340 nm ($\epsilon = 900$ L mol^{-1} cm^{-1}). **B** itself has a maximum at 360 nm ($\epsilon = 1.10 \times 10^3$ L mol^{-1} cm^{-1}). This

(17) Herrmann, W. A. *Angew. Chem., Int. Ed. Engl.* **1988**, *27*, 1297.
(18) Herrmann, W. A.; Kuchler, J. G.; Weichselbaumer, G.; Herdtweck, E.; Kiprof, P. *J. Organomet. Chem.* **1989**, *372*, 351.
(19) Binstead, R. A.; Zuberbühler, A. D. *Specfit*; Spectrum Software Associates, P.O. Box 4494, Chapel Hill, NC 27515.

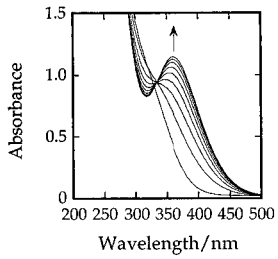

Figure 10. Repetitive spectral changes at 5 min intervals for the formation of **B** in THF from MTO via **A**. The first spectrum does not coincide with the isosbestic point, since the MTO to **A** conversion is still in progress. Conditions: [MTO] = 1.0 mM, [H_2O_2] = 0.20 M, and 25.0 ± 0.2 °C.

Scheme 3

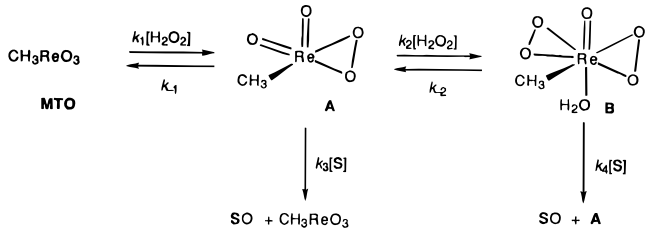

is close to values we have found in earlier work,[20] but considerably larger than one literature value[15] of 700 L mol^{-1} cm^{-1}.

Discussion

The results on catalyst deactivation can be interpreted by means of a relatively small number of chemical reactions. They are summarized in Scheme 1, which presents all of the reactions that are of importance in the MTO−H_2O_2 system. The essence of the reaction scheme is as follows: MTO and H_2O_2 form two species that contain rhenium and peroxide in 1:1 and 1:2 ratios, **A** and **B**. Under the conditions used, the two peroxide-binding reactions can be treated as rapid prior equilibria, even though in catalytic systems they are kinetic steps.

The irreversible destruction of the catalyst to give methanol and perrhenate proceeds via compound **A** or an analogous rhenium hydroperoxide complex, [$CH_3Re(\eta^1$-OOH)$(O_3)]^-$. Compound **B**, on the other hand, releases molecular oxygen, thereby restoring MTO, the parent form of the catalyst. That is to say, decomposition of **B** does not really destroy the catalyst, although it does decompose a corresponding amount of peroxide.

Neglected Reactions. The reactions shown in Scheme 1 suffice to account for all the observations. Other chemical equations can be written; at face value, they might appear to be as plausible as the ones given, yet they do not participate. For example, the answer is "no" to the question of whether **B**, like **A**, will release methanol, and "no" again to the question of whether **A**, like **B**, will release oxygen. Put more precisely, the two alternatives can be demonstrated to be of negligible importance compared to the ones found. The finding that **A** and **B** undergo distinctive reactions is intriguing, because, when it comes to their role in catalysis, **A** and **B** act as virtual stand-ins for one another. We have shown that, with few exceptions,[5,21] each peroxorhenium compound transfers a peroxidic oxygen to a given substrate with comparable kinetic efficiency. To illustrate this point, refer to Scheme 3, which gives the essence of the catalytic cycle.

Indeed, one of the messages we have presented previously is that the rate constants for the oxygen-transfer reactions of the two intermediates **A** and **B** are nearly the same. Following, for example, are values of k_3 and k_4 for a few typical oxygen-accepting substrates that suffice to make the point:[2−4,6]

substrate	k_3/(L mol^{-1} s^{-1})	k_4/(L mol^{-1} s^{-1})
$C_6H_5SCH_3$	2.65×10^3	0.97×10^3
Br^-	3.5×10^2	1.9×10^2
PPh_3	7.3×10^5	21.6×10^5
$PhCH{=}CMe_2$	1.00	0.70

Clearly, **A** and **B** exhibit comparable catalytic reactivities for a given substrate. That is not to say, of course, that a comparable concentration of product is produced from **A** and from **B** in any of these transformations. The contribution of each catalytic transfer step is defined not only by k_3 versus k_4, but also by the concentration of hydrogen peroxide and by the rate constants that characterize the formation of the active intermediates (k_1, k_{-1}, k_2, and k_{-2}). A combination of these quantities determines the proportion of each peroxorhenium species present in the system and its conversion to product. The extent of the two O atom transfer processes is determined by the peroxide concentration and all six rate constants, not simply k_3 and k_4. Moreover, the thermodynamic binding constants K_1 and K_2 are of less relevance than the constituent rate constants, since the peroxide binding steps are not instantaneous under catalytic conditions, but are kinetically competitive.

One means of gaining insight into the decompositions, where **A** and **B** behave so differently, is to examine what would happen were the role of each to be interchanged in the respective processes. For example, were **B** to release methanol upon attack by hydroxide ion, the chemical equation would be

$$CH_3Re(O)(O_2)_2 + OH^- \nrightarrow CH_3OH + [Re(O)_3(O_2)]^- \quad (23)$$

This reaction offers an unappealing prospect, however, in contrast with the corresponding one for **A** in Scheme 1, since the trioxo(peroxo)rhenate(VII) ion is not a known or stable species. Indeed, we have found that mixtures of ReO_4^- and H_2O_2 show no indication of peroxo complex formation, whereas the corresponding combination of CH_3ReO_3 and H_2O_2 readily results in the formation of **A**. So our contention is that reaction 23 is not important because it would give rise to a thermodynamically unfavorable product.

For a similar reason, we rationalize the lack of oxygen evolution from **A**:

$$CH_3Re(O)_2(O_2) \nrightarrow CH_3ReO_2 + O_2 \quad (24)$$

This event, were it to occur, would produce a rhenium(V) product. While this substance is known, oxygen atom abstraction from MTO takes a species with a very avid affinity for oxygen (e.g., PPh_3 and H_3PO_2);[22,23] in such cases CH_3ReO_2 can be formed slowly.[23−25] It seems unlikely, however, that conversion of peroxide to dioxygen can bring about this transformation. As to the parallel event that **B** undergoes (refer to the k_B step in Scheme 1), the bis(peroxo) species upon oxygen release generates a stable rhenium(VII) product, MTO itself. That is to say, one peroxide anion of **B** is released as elemental oxygen, and the other is converted into a pair of O^{2-} ions that are automatically incorporated into the newly-formed MTO. This

(20) Yamazaki, S.; Espenson, J. H.; Huston, P. *Inorg. Chem.* **1993**, *32*, 4683.

(21) One exception appears to be the cobalt thiolate complex $(en)_2Co(SCH_2CH_2NH_2)^{2+}$, for which $k_3 \gg k_4$.

(22) Holm, R. H.; Donahue, J. P. *Polyhedron* **1993**, *12*, 571−589.

(23) Abu-Omar, M. M.; Espenson, J. H. *Inorg. Chem.* **1995**, *34*, 6239.

(24) Herrmann, W. A.; Roesky, P. W.; Wang, M.; Scherer, W. *Organometallics* **1994**, *13*, 4531.

(25) Zhu, Z.; Espenson, J. H. *J. Mol. Catal.* **1995**, *103*, 87.

is how the more energetic Re(V) is avoided when **B** evolves oxygen. If **A**, however, were to disproportionate H_2O_2 like **B** does, it would necessarily require a bimolecular pathway, which would be unlikely considering the low concentrations of **A** at equilibrium.

The process for oxygen release has just been described in somewhat simplistic terms, with the goal in mind of rationalizing the absence of two decomposition pathways. In fact, there are some very fundamental matters that need to be addressed about the reactions that do take place. The timing of the events for oxygen release from **B** and the chemical mechanism by which MTO is released are examples. The balance of the discussion focuses on these events and on plausible mechanisms by which methanol and perrhenate are released.

Oxygen Evolution from B. The evolution of oxygen upon decomposition of **B** to MTO is one of the reactions shown in Scheme 1. In practice the yield of O_2 is rather low compared to $[\mathbf{B}]_0$, the reason being the relative values of $k'_{\mathbf{A}}$ (k'_{MTO}) and $k'_{\mathbf{B}}$. The decomposition of **B** occurs relatively slowly. The electrochemical determination of O_2 buildup showed that $[O_2]_\infty$ increased linearly with $[H_2O_2]_0$. This substantiates that **B** is the source of oxygen, as given by the kinetic scheme and eq 18 once the peroxide dependence of $f_{\mathbf{A}}$ (or f_{MTO}) is taken into account. The experimental rate constants obtained for O_2 release at various concentrations of $[H_2O_2]$ decreased hyperbolically as $[H_2O_2]$ increased; see Figure 4. This agrees with eq 13 and with the spectrophotometric kinetic measurements, Figure 3.

Precedents for oxygen release from η^2-peroxides are not very common. A bis(η^2-peroxo)(porphyrin)molybdenum(VI) is photochemically converted to oxygen and the *cis*-(dioxo)(porphyrin)molybdenum(VI).[9] Although the mechanism has not been established, an intermediate Mo^{IV}−peroxo complex has been proposed.[26] This is analogous to the mode of decomposition by which we propose **B** reverts to the parent MTO.

On the other hand, the rhenium(V)−peroxo complex $(HBpz_3)$-$Re(O)(O_2)$ decomposes to $(HBpz_3)ReO_3$ bimolecularly, rather than losing O_2 directly.[10] The authors attribute the failure of dioxygen release from a single site, despite a substantial driving force, to a symmetry restriction against the interconversion of a d^2 metal peroxide to a d^0 metal dioxo species. If this symmetry-derived restriction is general to all d^2 complexes, the decomposition of **B** to MTO and O_2 would proceed via a concerted mechanism rather than a stepwise transformation that involves a rhenium(V) peroxo intermediate.

Methanol Formation. Since the two possible pathways for the production of methanol (Scheme 1) cannot be resolved further on the basis of kinetics, and the labeling studies were inconclusive due to the oxygen exchange of perrhenate, we will discuss the molecular mechanisms by which each pathway may proceed. The decomposition of **A** may occur by the direct attack of OH^- on the methyl group of **A**, in effect, an S_N2 displacement, eq 27 or 28. Alternatively, a species with OH^- coordinated to rhenium may be responsible, which is represented by the following steps:

$$\mathbf{A} + H_2O \overset{K_a^{\mathbf{A}}}{\rightleftharpoons} \mathbf{A}{-}OH^- + H^+ \qquad (25)$$

$$\mathbf{A}{-}OH^- \xrightarrow{k_{25}} CH_3OH + {ReO_4}^- \qquad (26)$$

with $k_{\mathbf{A}} = k_{25}K_a^{\mathbf{A}}/K_w$, which affords $k_{25}K_a^{\mathbf{A}} = 6.2 \times 10^{-5}$ mol L^{-1} s^{-1}. If we approximate $K_a^{\mathbf{A}}$ as equal to K_a^{MTO} (1.2×10^{-12} mol L^{-1}; see eq 21), then $k_{25} = 5 \times 10^7$) s^{-1}. This is not an implausible formulation, save for the fact that eq 26 does not seem to represent particularly well the molecular changes that might lead to methanol.

Returning to the first formulation, in which OH^- attacks nucleophilically at the methyl group, either we envisage that this step leads directly to the products, in which case the requisite electronic rearrangement of the η^2-peroxide group is presumed to be relatively rapid, eq 27, or we invoke a sequential process in which a first-formed peroxorhenium(V) intermediate yields the final products after internal electron shifts, eq 28.

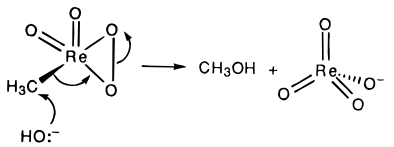

(27)

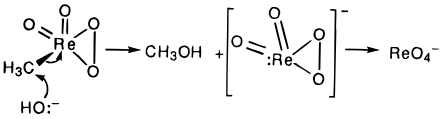

(28)

The alternative route for production of methanol and perrhenate ions involves the attack of HO_2^- on MTO. This proceeds most likely via a rhenium−hydroperoxo complex that is analogous to compound **A**, eq 29. Following its coordination

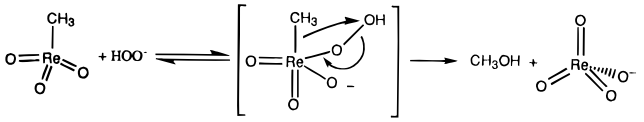

(29)

to the rhenium(VII) center, the hydroperoxide ligand becomes electrophilically activated and more susceptible to attack by the methyl group bound to rhenium. The outcome of this rearrangement (as illustrated by eq 29) is the elimination of methanol, leaving behind perrhenate as the final rhenium product.

Although neither kinetics nor labeling experiments were successful in discriminating between mechanisms 27 and 28 on the one hand and mechanism 29 on the other, a comment on which pathway would be more chemically sound based on our present knowledge is in order at this stage. Since $k_{\mathbf{A}}$ and k_{MTO} are close to the diffusion limit and the hydroperoxide anion is notably more nucleophilic than hydroxide,[27] one expects to see diffusion-controlled peroxide-induced rather than hydroxide-induced decomposition. Therefore, in light of these considerations and the fact that dilute MTO solutions without H_2O_2 persist for days in aqueous solution, we are inclined to favor the mechanism shown in eq 29 as the route by which the catalyst is irreversibly deactivated.

A precedent relating to the decomposition of MTO is the formation of $(Bu^tO)_2Mo(O)_2$ from the reaction of $Mo(OBu^t)_4$ with molecular oxygen in dilute solutions.[28] In concentrated solution, however, the product is $(Bu^tO)_4MoO$, from bimolecular oxygen activation. The dilute reaction appears to be unimolecular, as in eq 30.

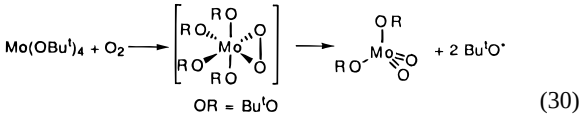

(30)

(26) Ledon, H. J.; Bonnet, M.; Gillard, D. *J. Am. Chem. Soc.* **1981**, *103*, 6209.

(27) Carey, F. A.; Sundberg, R. J. *Advanced Organic Chemistry*, 3rd ed.; Plenum Press: New York, 1990; Part A, p 268.

(28) Chisholm, M. H.; Folting, K.; Huffman, J. C.; Kirkpatrick, C. C. *Inorg. Chem.* **1984**, *23*, 1021.

Table 2. Summary of Equilibrium and Rate Constants at 25 °C

reaction	symbol	value
$CH_3ReO_3 + H_2O_2 \rightleftarrows CH_3Re(O)_2(O_2)(\mathbf{A}) + H_2O$	K_1	16.1 ± 0.2 L mol^{-1}
$\mathbf{A} + H_2O_2 \rightleftarrows CH_3Re(O)(O_2)_2(OH_2)(\mathbf{B})$	K_2	132 ± 2 L mol^{-1}
$CH_3ReO_3 + H_2O \rightleftarrows CH_3ReO_3(OH)^- + H^+$	K_a^{MTO}	$(1.2 \pm 0.2) \times 10^{-12}$ mol L^{-1}
$CH_3ReO_3 + OH^- \rightarrow ReO_4^- + CH_4$[a]	k_5	$(2.7 \pm 0.3) \times 10^{-2}$ L mol^{-1} s^{-1}
$CH_3ReO_3(OH)^- \rightarrow ReO_4^- + CH_4$[a]	k_6	$(2.2 \pm 0.1) \times 10^{-4}$ s^{-1}
$\mathbf{A} + OH^- \rightarrow CH_3OH + ReO_4^-$ [b]	$k_{\mathbf{A}}$	$(6.2 \pm 0.2) \times 10^{9}$ L mol^{-1} s^{-1}
$CH_3ReO_3 + HO_2^- \rightarrow ReO_4^- + CH_3OH$[b]	k_{MTO}	$(4.1 \pm 0.1) \times 10^{8}$ L mol^{-1} s^{-1}
$\mathbf{B} + OH^- \rightarrow CH_3ReO_3 + O_2$[c] $+ OH^-$	$k_{\mathbf{B}}$	2×10^{7} L mol^{-1} s^{-1}

[a] The reaction represented by k_5 is written in an alternative form represented by k_6. [b] $\mu = 0.010$ M and 25 °C. [c] pH 3.21, $\mu = 0.10$ M, and 25 °C.

Scheme 4

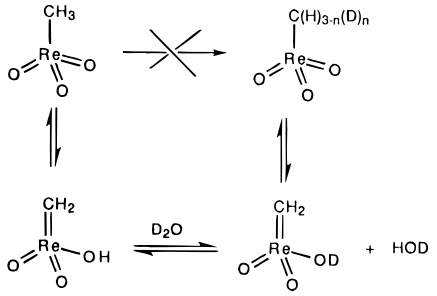

Any mechanism that would involve deprotonation of the methyl group is disregarded because deuterium incorporation into MTO does not occur in D_2O, Scheme 4. The lack of hydrogen exchange for deterium in D_2O deems the carbene tautomer of MTO insignificant.

Methane Formation. The decomposition of (peroxide-free) CH_3ReO_3 in alkaline solutions produces methane quantitatively. The kinetic and spectroscopic data show that an intermediate is "instantly" formed between MTO and hydroxide ions. This is reasonably a coordination compound, analogous to the adducts formed between MTO and chloride ions and nitrogen bases.[29] The short sequence of subsequent events that leads to methane formation can easily be depicted, as in eq 31.

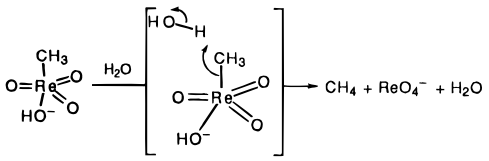

(31)

Formation of A and B. The equilibrium constants K_1 and K_2 were previously determined from absorbance readings at selected wavelengths.[6,20] The redeterminations given here were based on a global fitting routine[19] that in effect uses the continuous spectra. This treatment not only resulted in improved values and statistics for the equilibrium constants, but was also able to resolve the spectrum of **A**. Except at the lowest peroxide concentrations, the equilibrium situation is such that **A** in water is present at relatively low levels compared to MTO and **B**.

(29) Herrmann, W. A.; Kuchler, J. G.; Kiprof, P.; Riede, J. *J. Organomet. Chem.* **1990**, *395*, 55.

Scheme 5

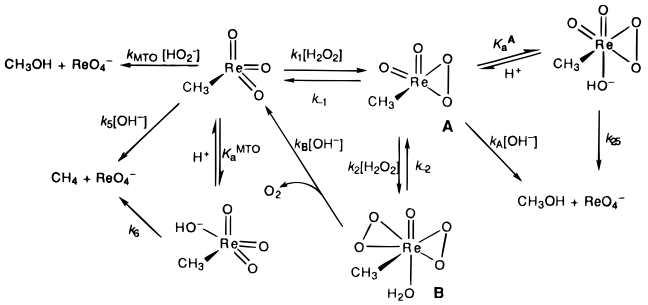

The spectrum of **A** could be obtained independently in THF, where the formation reactions for **A** and **B** are much slower than in water. Although the spectrum of **A** in water from SPECFIT fitting does not match exactly with that measured in THF, they are in reasonable agreement considering the procedures and fitting errors.

We contend that the monoperoxorhenium compound **A** was incorrectly identified in the NMR spectrum previously.[15] It seems likely to us that the reported chemical shift can be attributed to methanol, a decomposition product.

The rates at which methanol is produced and **B** decomposed are very sensitive to the solvent and pH. In both aqueous and semiaqueous environments, these compounds are stabilized by acid. In neat organic solvents the peroxides form more slowly than in water, and their temporal stabilities are greatly enhanced. For example, at pH 2 in water, the experimental rate constant is 6.2×10^{-3} s^{-1} whereas in THF it is 3.1×10^{-4} s^{-1}. As a result **B** is stable in the presence of excess peroxide for days in organic solvents, whereas 1 M acid is required to stabilize **B** comparably in water.

Summary. The important reactions are shown together in Scheme 5, and the rate and equilibrium constants are given in Table 2.

Acknowledgment. This research was supported by the U.S. Department of Energy, Office of Basic Energy Sciences, Division of Chemical Sciences, under Contract No. W-7405-Eng-82. P.J.H. is indebted to the administration and Board of Trustees of Northwestern College (Iowa) for their award of sabbatical leave. We are grateful to Kamel Harrata for the mass spectra determinations. J.H.E. is grateful to S. N. Brown and J. E. Bercaw for helpful comments.

JA952305X